Title:

Natural pretreatment and passive remediation of highly polluted acid mine drainage

Authors:

Francisco Macías[a*], Manuel A. Caraballo[a], José Miguel Nieto[a], Tobias S. Rötting[b], Carlos Ayora[c]

[a] *Geology Department, University of Huelva, Campus "El Carmen", E-21071 Huelva, Spain.*

[b] *Department of Geotechnical Engineering and Geosciences, Technical University of Catalonia (UPC-Barcelona Tech), Jordi Girona 1-3, E-08034 Barcelona, Spain.*

[c] *Institute of Environmental Assessment and Water Research, CSIC, Jordi Girona 18, E-08034 Barcelona, Spain.*

*corresponding author:

francisco.macias@dgeo.uhu.es

Tel.: +34-95-921-9834; fax: +34-95-921-9810

Abstract

Acid mine drainage (AMD) from the Iberian Pyrite Belt has high acidity and metal concentrations. Earlier pilot experiments, based on limestone sand dispersed in wood shavings (dispersed alkaline substrate; DAS) have been shown to be an efficient treatment option. However, complete metal removal was not achieved, principally due to the high ferrous iron concentration in the inflow AMD. In order to oxidize and remove iron, a natural Fe-oxidizing lagoon (NFOL) was added prior to treatment with limestone-DAS. The NFOL comprises several preexisting Fe-stromatolite terraces and cascades, and a lagoon with a volume of 100 m^3 built near the mine shaft. Downstream of the NFOL, the limestone-DAS treatment consists of two reactive tanks of 3 m^3 each filled with limestone-DAS reactive substrate, connected in series with two decantation ponds of 6 m^3 each and several oxidation cascades. The AMD emerging from the mine shaft displayed a pH near 3, a net acidity of 1,800 mg/L as $CaCO_3$ equivalents, and mean concentrations of 440 mg/L Zn; 275 mg/L Fe (99% Fe(II)); 3,600 mg/L SO_4; 250 mg/L Ca; 100 mg/L Al; 15 mg/L Mn; 5 mg/L Cu; and 0.1–1 mg/L As, Pb, Cr, Cd, Co, and Ni. The oxidation induced in the NFOL enhanced ferric iron concentration, showing an average of 65% oxidation and 38% retention during the monitoring period. The whole system removed a mean of 1,350 mg/L net acidity as $CaCO_3$ equivalents (71% of inflow); corresponding to 100% of Fe, Al, Cu, Pb and As, and 6% of Zn.

Keywords

Iron oxidation, passive treatment, acid mine drainage, Iberian Pyrite Belt

1. Introduction

Acid Mine Drainage (AMD) is one of the main environmental problems caused by mining activities and has the potential to contaminate surface and ground water (Nyquist and Greger, 2009). In the Iberian Pyrite Belt (IPB) this pollution is widespread, being particularly severe in the Huelva region (southwestern Spain), where more than 60 different mines operated during the past century (Pinedo Vara, 1963). This mining activity has left a large number of abandoned pollution sources discharging AMD into the Tinto and Odiel river basins (Sáinz et al., 2002; Sarmiento et al., 2009). Both rivers flow into the Huelva estuary, which finally discharges to the Atlantic Ocean an average pollution of 7,900 t $year^{-1}$ of Fe, 5,800 t $year^{-1}$ of Al, 3,500 t $year^{-1}$ of Zn, 1,700 t $year^{-1}$ of Cu, and 1,600 t $year^{-1}$ of Mn, in addition to minor amounts of many other metals (e.g. Co, As, Ni, Pb, Cd) (Olías et al., 2006). Due to the large number of pollution sources, the difficulty of access to them, and the lack of legal responsibility by ancient mining companies (orphan sites), the use of passive remediation technologies has to be considered as an essential component of any ecological restoration to be developed in these highly polluted mining districts (Kalin, 2004).

Conventional passive treatment systems such as anoxic limestone drains (ALD; Hedin et al., 1994) or reducing and alkalinity producing systems (RAPS; e.g. Jage et al., 2001) have been tested in the IPB (López Fernandez et al., 2003; Rötting et al., 2005), showing serious problems of clogging and loss of reactivity when exposed to AMD with very high metal concentrations.

To solve these problems, dispersed alkaline substrate (DAS) has been developed (Rötting et al., 2008a) as a new reagent mixture that is composed of a fine-grained alkaline reagent (limestone sand or magnesium oxide powder) mixed with a coarse inert

matrix (pine wood shavings) to increase reactivity and reduce passivation, and to provide high porosity and reduce clogging problems, respectively.

Previous field experiments using limestone-DAS (Rötting et al., 2008b) or a combination of different steps with limestone-DAS and MgO-DAS reactive mixtures (Caraballo et al., 2009a) have shown significant effectiveness in Fe and Al removal, although complete Fe removal was not achieved after the limestone-DAS steps of any of these previous experiments. Rötting et al.'s (2008b) field experiment in Monte Romero employed one limestone-DAS reactive tank followed by two decantation ponds. This design, treating AMD with 280–380 mg/L of total Fe (95% Fe(II)), achieved 48% and 93% relative removal for Fe and Al, respectively. Caraballo et al.'s (2009a) field experiment added a second limestone-DAS reactive tank after the two decantation ponds of the previous treatment at Monte Romero, two new decantation ponds, and a final MgO-DAS reactive tank. Relative removal was increased to 58% Fe and 93% Al in the limestone-DAS steps of the treatment. This study also showed that for optimal performance of the MgO-DAS tank, complete Fe and Al removal has to be achieved after the limestone-DAS steps of the treatment. The main reason for the poor performance of the MgO reagent in the presence of Fe and Al was the fast development of an Fe-Al coating on the MgO (Cortina et al., 2003) and also to the significant decrease in hydraulic conductivity of the reactive material in response to Al precipitation (Caraballo et al., 2010).

This incomplete Fe removal in the limestone-DAS tanks is directly linked to the high Fe(II) concentration in the inflow AMD; with such Fe(II) values several successive limestone reactive tanks and decantation pond steps are necessary for complete removal of Fe.

92 Fe(II)-rich AMD systems are colonized by a broad range of Fe-oxidizing
93 bacteria that essentially contribute to the fast biogeochemical oxidation of Fe(II) to
94 Fe(III) (Kirby et al., 1999) and therefore have a key role in the natural attenuation of
95 AMD (Casiot et al., 2004; Johnson and Hallberg, 2003). This iron oxidation capacity
96 has been tested in iron-oxidizing bioreactors (Johnson and Hallberg, 2005). These
97 passive biological systems have achieved significant Fe oxidation values in packed bed
98 reactors, but their applicability for AMD remediation at field or industrial scale is
99 limited due to problems related to the immobilization of Fe-oxidizing bacteria in the
100 reactors (Long et al., 2003).

101 Fe(II) oxidation in aquatic systems can also be enhanced abiotically. The
102 surface-catalyzed oxidation of ferrous iron (SCOOFI) was first described by Best and
103 Aikman (1983). In this process, Fe(II) is absorbed on the surfaces of Fe(III)-hydroxides
104 and is oxidized in a catalytic reaction that is more rapid than open-water abiotic
105 oxidation (such as occurs in an aerobic wetland). This process has been applied in
106 unsaturated (Younger, 2000) and saturated environments (Younger et al., 2002) with
107 circum-neutral mine waters (pH ≈ 5), but it has not been implemented at large-scale in
108 low-pH AMD environments.

109 Settlement lagoons and aerobic wetlands are frequently used in passive
110 treatment systems to oxidize and remove Fe in net-alkaline ferruginous waters
111 (Sapsford and Watson, 2011; Younger et al., 2002), typically achieving Fe removal
112 rates of 10–20 g Fe/m^2·day. In current best practices for passive AMD treatment, lagoon
113 and wetland use with net-acidic mine water is highly discouraged (Mayes et al., 2009;
114 Younger et al., 2002). When used with net-acidic mine waters (Whitehead et al., 2005),
115 Fe removal efficiency in aerobic wetlands or lagoons has been found to be much lower
116 (6 g Fe/m^2·day).

Fe(II) oxidation and removal in naturally formed iron terraces and pools has been widely observed in the IPB (Asta et al., 2010; Caraballo et al., 2011). This natural attenuation relies on several processes, such as Fe oxidizing bacteria activity, catalytic oxidation of Fe(II) on the surface of Fe precipitates, water supersaturation with respect to schwertmannite, and abiotic Fe oxidation. The natural processes at work should be given due consideration before planning remediation processes (Hashim et al., 2011).

A new concept called natural Fe-oxidizing lagoon (NFOL) was tested in the present study. The philosophy of this AMD pretreatment is to enhance the iron-oxidation processes involved in the natural attenuation of the AMD pollution by recreating, at a larger scale, the naturally formed iron terraces and pools in the IPB. The implementation of this natural pretreatment prior to an DAS-based passive treatment system is expected to significantly improve water quality at the outflow of the system. The NFOL is expected to remove an important amount of Fe due to schwertmannite precipitation, increase Fe(III) concentration in the limestone passive treatment inflow water, and improve the passive treatment performance to achieve complete removal trivalent metals (mainly Fe and Al).

2. Materials and methods

2.1 Field site

The pilot treatment system was set up at the Monte Romero abandoned mine complex, located in Almonaster la Real, southwestern Spain (Figure 1A). The mine complex was operated between 1876 and 1967 by different mine companies to obtain Zn and Pb (Pinedo Vara, 1963). The ore was mined by underground operations from a massive pyrite deposit with minor amounts of Zn, Pb, and Cu sulfides, belonging to the

140 northern part of the IPB (Pinedo Vara, 1963). The enclosing rocks are low grade slates
141 and phyllites; carbonate rocks are absent in the region.

142 After the closure of the mine and the end of groundwater pumping, the mine
143 galleries and shafts flooded, resulting in the generation of AMD. During the study, the
144 AMD emerging from the main shaft displayed a pH near 3; a net acidity of 1,800 mg/L
145 as $CaCO_3$ equivalents; and mean concentrations of 440 mg/L Zn, 275 mg/L Fe (99%
146 Fe(II)), 3,400 mg/L SO_4, 250 mg/L Ca, 100 mg/L Al, 18 mg/L Mn, 5 mg/L Cu and 0.1–
147 1 mg/L As, Pb, Cr, Cd, Co, and Ni. These concentrations are one to two orders of
148 magnitude higher than those reported for a number of North American passive treatment
149 systems (Ziemkiewicz et al., 2003).

150 The system was monitored between April and September 2008, when the natural
151 flow of the mine shaft ceased due to the typical drought season in the south of Spain.
152 During the first months of operation the mean flow rate was 1.5 L/s, while in September
153 it started to decrease until the flow ceased.

154 ### 2.2 NFOL pretreatment and pilot scale passive treatment system description

155 Fe-stromatolites typically grow on small rimstone dams forming sequences of
156 cascades and pools (Figure 2A), where different processes are involved in Fe speciation
157 and precipitation. Fe-oxidizing bacteria play an important role in the Fe cycle in AMD
158 environments (Bigham and Nordstrom, 2000; Johnson and Hallberg, 2003). These
159 bacteria not only induce the generation of schwertmannite and other Fe precipitates on
160 the Fe-stromatolite surface, but also favor Fe removal along the flowing water course
161 and in the pools (Asta et al., 2010). As previously mentioned, the catalytic oxidation of
162 Fe on the Fe-precipitate surfaces is another important process involved in this metal
163 removal (Younger, 2000). Previous studies revealed the necessity of a very high

164 specific surface area in the Fe-precipitates to obtain an efficient application of the
165 SCOOFI process to a passive treatment system (Younger et al., 2002).

166 To recreate the Fe attenuation processes observed in nature on a larger scale and
167 to exploit them in a passive treatment system, a NFOL pretreatment was implemented
168 in the pilot scale passive treatment system at Monte Romero. The NFOL comprises an
169 upper section (close to the mine shaft) formed by several preexisting Fe-stromatolite
170 rimstone dams and cascades (Figure 2B) followed by a lagoon with a capacity of
171 approx. 100 m^3 (Figure 2C). A 100 cm high dam was built from soil and concrete blocks
172 and sealed with impermeable plastic liner to close a small valley in the vicinity of the
173 mine shaft (Figure 2C). The bottom and the pre-existing natural side walls of the valley
174 were not modified to keep the terrain irregularities (soil, rocks, shrubs and so on). These
175 irregularities offered a high specific surface area to increase the efficiency of the iron
176 oxidation and removal processes.

177 A pipe takes the AMD from the NFOL lagoon across the Monte Romero tailings
178 ponds to the inflow of the limestone-DAS treatment (Figure 1B). A schematic view of
179 the limestone-DAS passive treatment system is shown in Figure 1C. The system is
180 composed of two fiberglass tanks (T1 and T2) of 3 m^3 in volume each connected in
181 series with two decantation ponds (D1 and D2) of 6 m^3 in volume each. The tanks were
182 filled with the reactive mixture limestone-DAS, with 80% (v/v) pine wood shavings and
183 20% (v/v) limestone sand (1–5 mm of grain size), and were equipped with perforated
184 pipes and a 15 cm layer of quartz gravel in the bottom as a drain. Assuming a porosity
185 of at least 50%, the flow rate was set to 1,000 mL/min to obtain a residence time of 24 h
186 for T1 and T2, and 4 days for each decantation pond.

187 2.3 Water sampling and analysis

188 Water samples were taken at least twice a month at the following representative
189 points: mine shaft, outflow of the NFOL lagoon, inflow and outflow of the reactive
190 tanks (T1-in, T1-out, T2-in, and T2-out), and outflow of the decantation ponds (D1-out
191 and D2-out). Additional AMD samples were taken to analyze Fe(II) and total Fe for the
192 evaluation of Fe oxidation in the NFOL. Physical-chemical parameters were measured
193 in the field using specific portable meters. The pH and redox potential were determined
194 using a PH25 meter (Crison®) with Crison electrodes, and were controlled using 2
195 points (240 mV and 470 mV) for redox potential and calibrated with 3 points (4.01,
196 7.00, 9.21) for pH, with Crison standard solutions. The redox potential measurements
197 were corrected to the standard hydrogen electrode. Electrical conductivity and
198 temperature were measured using a CM35 meter (Crison®) with 3 calibration points
199 (147 and 1413 μS/cm, and 12.88 mS/cm). Dissolved O_2 was measured with an auto-
200 calibrating Hanna® meter. Gross alkalinity was determined using CHEMetrics® Total
201 Titrets®, with a range of 10–100 or 100–1000 mg/L as $CaCO_3$ equivalents.

202 Water samples were filtered immediately after collection through 0.1 μm
203 Millipore filters on Millipore syringe filter holders, acidified in the field to pH < 1 with
204 ultrapure HNO_3 and stored in the dark at 4 ºC in sterile polypropylene containers until
205 analyzed. Analyses were carried out in the Central Research Services of the University
206 of Huelva by inductively coupled plasma atomic emission spectrometry (ICP-AES,
207 Yobin-Ybon Ultima2). The method used was designed to estimate major, minor, and
208 trace elements in waters affected by AMD (Tyler et al., 2004). Detection limits were:
209 200 μg/L for Al, Fe, Mn, Mg, K, Si, and S; 500 μg/L for Ca; 50 μg/L for Zn; 5 μg/L for
210 Cu; 2 μg/L for As; and 1 µg/L for Cd, Co, Cr, Ni, Pb, Ti, and V; analytical error was
211 lower than 5%.

Fe(II) and total Fe were determined by colorimetry at 510 nm after complexation in the field by the addition of 0.5% (w/w) 1.10-phenanthrolinium chloride solution to the filtered sample (Rodier et al., 1996), using a DR/890 portable colorimeter (HACH®). The detection limit was 0.3 mg/L and precision was better than 5%; Fe(III) was calculated as the difference between total Fe and Fe(II).

Net acidity (Ac; mg/L as $CaCO_3$) was calculated according to the following equation (Kirby and Cravotta, 2005a, 2005b):

$$Ac = 50{,}045 \cdot (3 \cdot c_{Al} + 2 \cdot c_{Fe} + 2 \cdot c_{Mn} + 2 \cdot c_{Zn} + 10^{-pH}) - alk$$

where C_x is the molar concentration of Al, Fe, Mn and Zn (mol/L), and *alk* is the measured gross alkalinity (mg/L as $CaCO_3$ equivalents).

Relative metal removal (r) (%) was calculated as:

$$r = \frac{(c_{in} - c_{out})}{c_{in}} \cdot 100$$

where c_{in} is the inflow concentration (mg/L) and c_{out} is the outflow concentration (mg/L).

Saturation indices (SI = log IAP − log k; IAP = ion activity product) of possible minerals with respect to analyzed element concentrations were calculated using PHREEQC Interactive 2.15.0 (Parkhurst and Appelo, 1999) and the WATEQ4F database (Ball and Nordstrom, 1991). The schwertmannite solubility product was taken from Bigham et al. (1996).

2.4 Solid sampling and analysis

After the experiments concluded, a depth profile of each reactive tank was dug out to analyze the precipitates developed within the reactive substrate. Based on visual observation, the following samplings were taken: 0–1, 1–6, 6–11, 11–16, 16–21, 21–26, 26–31, 31–36, 36–45, and 45–100 cm depth for T1 and 0–2, 2–10, 10–20, 20–30, 30–40, and 40–100 cm depth for T2. An additional sample of fresh precipitates was collected in the NFOL lagoon.

To obtain the bulk chemistry of the precipitates formed in the reactive tanks and lagoon, the samples were digested with concentrated HNO_3. Metal concentrations of the different digestions were analyzed by ICP-AES (Yobin-Ybon Ultima2). Duplicate samples were used to validate the digestion results, the following maximun relative coefficients of variation were obtained: 5.2% for Al, 2.1% for As, 5.1% for Ca, 0.8% for Cu, 3.1% for Fe, 4.5% for Pb and 5.6% for S.

X-ray diffraction (XRD) patterns were obtained with a Bruker D5005 X-ray Diffractometer with Cu Kα. Diffractometer settings were 40 kV, 30 mA, a scan range of 3–65º 2θ, 0.02 2θ step size, and 2.4 s counting time per step.

3. Results and discussion

3.1 NFOL performance

During the study, the AMD in the lagoon was highly turbid and had a reddish-brown aspect (Figure 2C), indicating the presence of Fe(III) flocs throughout the entire water body. Physical-chemical parameters, water composition, and Fe speciation were fairly constant across depth profiles in the lagoon (data not shown), suggesting that the Fe oxidation took place in the whole volume of AMD. Through the operation time pH values oscillated between 2.6 and 2.8, close to the optimal conditions for Fe-oxidizing bacteria growth of pH values near 3 reported by Amaro et al. (1991). The dissolved

oxygen concentration increased from 7–10% in the emerging AMD to 40–50% in the lagoon. Fe oxidation was probably due to bacterial activity, because the abiotic oxidation is very slow at these pH values (Singer and Stumm, 1970; Bigham and Nordstrom, 2000). Although microbial diversity data were not obtained in this study, the importance of Fe-oxidizing bacteria (e.g. *Acidithiobacilus ferrooxidans*) in the oxidation of Fe(II) to Fe(III) is widely recognized (e. g. Baker and Banfield, 2003; Kirby et al., 1999). Other Fe oxidation processes, however, cannot be discounted (e.g., SCOOFI process). The increase of dissolved oxygen also promotes iron precipitation in the next steps of the treatment.

Time evolution of Fe speciation in the emerging AMD and the lagoon for the first four months of operation can be observed in Figure 3. The amount of Fe removed by the NFOL was calculated by subtracting the total Fe concentration in the lagoon from the total Fe concentration in the mine shaft. The values obtained were referred to as "Fe(III) removed" (Figure 3) on the basis of the mineralogical characterization performed in this study, which only showed schwertmannite and goethite as the precipitate forming minerals. As can be observed in Figure 3, total Fe concentration ranged from 300 to 240 mg/L in the mine shaft. Fe(II) was clearly the dominant species in the emerging water from the mine shaft. The oxidation induced in the cascades and lagoon significantly increased Fe(III) concentration and removal in the lagoon, showing an average value of 92 mg/L of Fe(III) generated in the NFOL. As can be observed in Figure 3, there is an important increase in the percentage of Fe(III) in the total Fe concentration in the lagoon, changing from 42% in April to 89% in July. For the same period, an increase in Fe removal was also observed, evolving from 18% to 45% of the total Fe concentration in the mine shaft. These effects could be explained by an increase in the specific surface of the pretreatment and subsequently increased nucleation

surfaces for the growth of new Fe precipitates. The increase of Fe-oxidizing efficiency may also be linked to higher Fe-oxidizing bacteria activity during summer.

The saturation indexes showed that the water in the lagoon is supersaturated in schwertmannite and goethite (Table 1). However, the only mineral phase detected by XRD in fresh precipitates generated in the lagoon was schwertmannite, ruling out the direct formation of goethite in these waters. The mineralogical composition of the Fe-stromatolites developed in Monte Romero was previously studied by Acero et al. (2006). Their study detected the presence of schwertmannite as the main neoformed Fe mineral phase and goethite as an aging product of the former.

Chemical composition of the fresh precipitates in the NFOL lagoon showed high concentrations of Fe and S (Table 2), as expected for pure schwertmannite. On the basis of this analysis, schwertmannite stoichiometry was deduced to be $Fe_8O_8(OH)_{4.6}(SO_4)_{1.7}:nH_2O$. The sulfate value is slightly lower than the one proposed by Acero et al. (2006) for schwertmannite in Monte Romero Fe terraces, and slightly higher than those found by Bigham et al. (1996). The very high concentration of As in schwertmannite (Table 2) is consistent with the observed As removal from the AMD (Table 1) and confirms that the NFOL pretreatment is an important sink for As.

To obtain a better understanding of the NFOL efficiency, some design parameters and Fe removal rates from lagoons and aerobic wetlands in the world are shown in Table 3. The NFOL was built following the recommendations offered by PIRAMID-Consortium (2003) according to surface area (m^2) and inflow (L/s) for settlement lagoons, but facing an inflow Fe concentration 5 times higher than the original specifications. A recent study in net-alkaline mine drainage encouraged the abandonment of $g/m^2/day$ as both a lagoon design criterion and Fe removal efficiency

parameter (Sapsford and Watson, 2011). However, the use of this ratio in acid mine drainage, although in need of revision, is strongly established (Younger, 2002; PIRAMID-Consortium, 2003).

Aerobic wetlands and lagoons are commonly employed in the passive treatment of net-alkaline metal polluted waters due to their higher efficiency in these environments. As the processes involved in the remediation of net-alkaline and net-acidic metal polluted water in aerobic wetlands and lagoons are very similar, it was decided to use both of them to compare with the results obtained in the NFOL in Monte Romero (Table 3). As can be observed, the highest Fe removal reported in lagoons treating net-alkaline waters is 26 g/m^2/day (Hedin, 2008; Kruse et al., 2009) while aerobic wetlands treating net-acidic waters only achieved 6 g/m^2/day (Whitehead et al., 2005). The NFOL pretreatment showed a mean Fe removal as high as 100 g/m^2/day over the study period, 4 to 16 times higher than the Fe removal observed in other conventional treatments. This value is one order of magnitude higher than the common standards for the efficient operation of a lagoon or an aerobic wetland in AMD environments.

3.2 Limestone-DAS treatment

During the monitored period there were no sudden changes in physical-chemical parameters or hydrochemical values in the limestone-DAS system. In the output of T1, pH and gross alkalinity displayed values of 5.9–6.2 and 210–260 mg/L as $CaCO_3$ equivalents, respectively, showing only slight oscillations, probably related to variations in the input flow rate caused by partial clogging of the pipe connecting the NFOL and T1 (Figure 1B). In the output of T2 these parameters were even more stable, with pH values of 6.6 and 150 mg/L of gross alkalinity as $CaCO_3$ equivalents. Only during the

first two months of operation, some Fe (35 mg/L) was detected in the output of T1, probably due to the high Fe concentration at the mine shaft (Figure 3). During this time, the Fe residual from T1 was eliminated in T2. For the rest of the time, Fe was completely retained in T1.

As can be observed in Figure 4, the main changes in AMD hydrochemistry occur in the T1 reactive tank, where pH increased from 2.6 to 6.1 and more than 200 mg/L as $CaCO_3$ equivalents of gross alkalinity were measured in the outflow. This tank also decreased Fe and Al concentrations from 150 mg/L to 30 mg/L and from 100 mg/L to 10 mg/L, respectively. The remaining Fe in the output of T1 was predominantly Fe(II). In the subsequent cascades and decantation ponds Fe(II) was oxidized (favored by the increase in water pH after limestone dissolution) and removed. Fe hydrolysis and precipitation is responsible for the alkalinity consumption observed in the decantation ponds (Figure 4). During the entire period of study, no Fe or Al was detected in the output of T2.

After the conclusion of the experiment, two horizons rich in Fe and Al, respectively, were observed in the reacted material. The bulk chemistry of the solid samples obtained in both reactive tanks is shown in Table 2. The Fe-rich horizon is restricted to the upper 6 cm of reactive material, with a strong accumulation between 0 and 1 cm depth. The XRD study performed on these samples only revealed the presence of goethite. However, goethite has been observed as an aging product of schwertmannite, the main fresh precipitate observed in a detailed study of the Fe horizon in a limestone-DAS tank in a previous experiment (Caraballo et al., 2009b). An Al-rich horizon was detected between 1 cm and 16 cm depth (Table 2). Even though basaluminite and gibbsite were supersaturated at the output of T1 (Table 1), the diffractograms only revealed the presence of gypsum as a neoformed phase, and calcite

354 from the initial reactive substrate. Probably Al was present as an amorphous phase,
355 which was not detected by XRD. From 16 cm to the bottom of the tank only calcite was
356 present; this part of the tank can be considered unreacted material, indicating that the
357 treatment performance could have been maintained for a much longer time than the
358 study period.

359 As a result of the very small amount of Fe and Al treated by T2, only gypsum
360 was detected by XRD as a newly formed mineral in the upper part of the reactive
361 substrate. The bulk chemistry of the solid samples obtained from T2 show the retention
362 of Fe and Al in the upper 10 cm of the reactive material (Table 2). Calcite is the only
363 phase detected by XRD from 10 cm to the bottom of the reactive tank, and calcium
364 concentration in the solid samples remains close to 340 mg/g. Therefore, the reactive
365 material from 10 cm to the bottom of the T2 tank can be considered unreacted substrate.
366 A significant difference observed between T2 and T1 is the higher amount of Zn
367 removed in T2 (Table 2). This removal is probably related to the higher pH values
368 reached in T2 (Figure 4), which would increase the efficiency of the adsorption
369 processes involved in removal of this metal.

370 ### 3.3 Metal removal efficiency

371 In order to evaluate the metal removal efficiency obtained in the present work
372 and how the NFOL pretreatment improved the limestone-DAS passive treatment
373 performance, metal removal data from similar field experiments carried out in Monte
374 Romero by Rötting et al. (2008b) and Caraballo et al. (2009a) are compared with the
375 present study (Figure 5).

376 During the entire operation time of the present study a complete removal of Fe
377 and Al was achieved. In addition, Cu, As, and Pb were also completely eliminated. Fe

and As were the only elements partially retained in the NFOL (Figure 5, section 1), achieving an elimination of 38% for Fe and 80% for As. The high Fe removal efficiency of the NFOL is an important achievement in itself. Another important effect of the NFOL in the passive treatment performance is the capacity of the NFOL to oxidize Fe(II) (Figure 3). The high Fe(III) concentration in the input of the first limestone-DAS tank (section 2) promotes a noticeably large Fe removal in the tank, reaching 180 mg/L (59%), whereas experiments A and B only achieved Fe removals of 150 mg/L (48%) and 120 mg/L (34%), respectively (Figure 5). The presence of Fe(III) causes the precipitation of schwertmannite inside the tank, consuming OH^- and producing new acidity, which enhances calcite dissolution and the efficiency of the treatment. It is important to note that, in this study, section 2 achieved a higher percentage of Fe retention compared with sections 2 and 3 together in experiment B, and a very similar removal in absolute terms. This suggests that the NFOL pretreatment (section 1) markedly improves the limestone-DAS performance for Fe removal. Most of the Al (98%) and all the Cu and Pb were removed in section 2 in this work whereas experiment A did not attain total Al, Cu, and Pb removal and experiment B only achieved similar values after the retention of these metals in section 3 (Figure 5). The second limestone-DAS tank (section 3) in the present study removed the residual Fe and Al not retained by section 2 (Figure 5). The comparison of these observations with experiment B suggests that NFOL pretreatment not only improves Fe retention in the limestone-DAS tank, but it also indirectly increases Al, Cu, and Pb removal.

Only a small amount of Zn retention was observed in section 3. The efficient removal of Zn would probably require a reactive material supplying pH values higher than those obtained with calcite (Rötting et al., 2008c). Treatment of the water leaving T2 with MgO-DAS is currently in progress.

403 Net acidity is a good parameter to evaluate the efficiency of a treatment system
404 with regard to metal removal and water quality improvement. In the present study the
405 entire system achieved a net acidity removal of 1,350 mg/L as $CaCO_3$ equivalents, 71%
406 of the input net acidity; whereas in the experiment of Rötting et al. (2008b) and
407 Caraballo et al. (2009a) net acidity removals of only 870 mg/L (56%) and 730 mg/L
408 (30%) as $CaCO_3$ equivalents, respectively, were attained. Therefore, the implementation
409 of the NFOL pretreatment has significantly increased the overall efficiency of the
410 passive treatment system, achieving a net acidity removal almost two times higher than
411 those attained in previous passive treatment schemes based on limestone-DAS alone.

412 **4. Conclusions**

413 For the first time, Fe and Al have been removed completely from highly metal
414 polluted AMD in the IPB using a passive treatment system. During the study period, the
415 NFOL pretreatment oxidized an average of 65% of the inflowing Fe(II), precipitated a
416 mean 38% of total inflowing Fe, and achieved an Fe removal rate around 100 $g/m^2/day$,
417 ten times higher than the common standards for the efficient operation of lagoons in
418 net-acidic environments. Additionally, more than 80% of As from the inflow water was
419 retained. The whole system (NFOL+DAS) was able to remove a net acidity of 1,350
420 mg/L as $CaCO_3$ equivalents from a total net acidity of 1,800 mg/L as $CaCO_3$
421 equivalents at the mine shaft (71%), which corresponds to a relative removal of 100%
422 Fe, Al, Cu, Pb, and As and 6% of Zn.

423 These results demonstrate that the coupled application of NFOL pretreatments
424 and limestone-DAS passive treatments is a feasible and promising remediation option to
425 treat highly contaminated AMDs. The small land surface requirement, high Fe oxidation
426 and removal achieved, simple design, low-cost implementation, and infrequent

maintenance are some key features of the NFOL that make this pretreatment a promising remediation option to be incorporated in more complex passive treatment systems in AMD affected regions.

5. Acknowledgements

This study was funded by the Spanish Government project CGL2010-21956-C02-02. F. Macías was financially supported by the Spanish Government with a FPI PhD fellowship. We thank the analytical assistance of Rafael Carrasco, María José Ruiz and Mari Paz Martin from the Central Research Services of the University of Huelva.

6. References

Acero, P., Ayora, C., Torrento, C., Nieto, JM., 2006. The behavior of trace elements during schwertmannite precipitation and subsequent transformation into goethite and jarosite. Geochim. Cosmochim. Ac. 70 (16), 4130-4139.

Amaro, A.M., Chamorro, D., Seeger, M., Arrendondo, R., Perrano, I., Jerez, C.A., 1991. Effect of external pH perturbations on in vivo protein synthesis by the acidophilic bacterium Thiobacilus ferrooxidans. J. Bacteriol. 173, 910-915.

Asta, M.P., Ayora, C., Román-Ross, G., Cama, J., Acero, P., Gault, A.G., et al. 2010. Natural attenuation of arsenic in the Tinto Santa Rosa acid stream (Iberian Pyritic Belt, SW Spain): The role of iron precipitates. Chem. Geol. 271 (1-2), 1-12.

Baker, B.J., Banfield, J.F., 2003. Microbial communities in acid mine drainage. FEMS Microbiol. Ecol. 44, 139-152.

Ball, J.W., Nordstrom, D.K., 1991. User's Manual for WATEQ4F with Revised Thermodynamic Database and Test Cases for calculating Speciation of Major,

Trace and Redox Elements in Natural Waters, U.S. Geological Survey Water Resources Investigation. pp. 91-183,

Best, G.A., Aikman, D.I., 1983. The treatment of ferruginous groundwater from an abandoned colliery. Water Pollut. Control. 82 (4), 537-566.

Bigham, J.M., Nordstrom, D.K., 2000. Iron and aluminum hydroxysulfates from acid sulfate waters, in: C.N. Alpers, J.L. Jambor, D.K. Nordstrom (Eds.), Sulfate minerals: Crystallography, Geochemistry, and Environmental Significance, vol. 40, Reviews in Mineralogy and Geochemistry, Mineralogical society of America, Chantilly, Virginia. pp. 351–403.

Bigham, J.M., Schwertmann, U., Traina, S.J., Winland, R.L., Wolf, M., 1996. Schwertmannite and the chemical modeling of iron in acid sulfate waters. Geochim. Cosmochim. Ac. 60 (12), 2111-2121.

Caraballo, M.A., Rötting, T.S., Macías, F., Nieto, J.M., Ayora, C., 2009a. Field multi-step calcite and MgO passive system to treat acid mine drainage with high metal concentration. Appl. Geochem. 24, 2301-2311.

Caraballo, M.A., Rötting, T.S., Nieto, J.M., Ayora, C. 2009b. Sequential extraction and DXRD applicability to poorly crystalline Fe- and Al-phase characterization from an acid mine water passive remedation system. Am. Mineral. 94, 1029-1038.

Caraballo, M.A., Rötting, T.S., Silva, V., 2010. Implementation of an MgO-based metal removal step in the passive treatment system of Shilbottle, UK: Column experiments. J. Hazard. Mater. 181, 923-930.

Caraballo, M.A., Sarmiento, A.M., Sanchez-Rodas, D., Nieto, J.M., Parviainen, A. 2011. Seasonal variations in the formation of Al and Si rich Fe-stromatolites in the highly polluted acid mine drainage of Agua Agria Creek (Tharsis, SW Spain). Chem. Geol. doi:10.1016/j.chemgeo.2011.02.012

475 Casiot, C., Bruneel, O., Personné, J.C., Leblanc, M., Elbaz-Poulichet, F., 2004. Arsenic
476 oxidation and bioaccumulation by the acidophilic protozoan, Euglena mutabilis,
477 in acid mine drainage (Carnoulès, France). Sci. Total. Environ. 320(2-3): 259-
478 267.
479 Cortina, J.L., Lagreca, I., De Pablo, J., Cama, J., Ayora, C., 2003. Passive In Situ
480 Remediation of Metal-Polluted Water with Caustic Magnesia: Evidence from
481 Column Experiments. Environ. Sci. Technol. 37 (9), 1971-1977.
482 Hashim, M.A., Mukhopadhyay S., Sahu J.N., Sengupta B., 2011. Remediation
483 technologies for heavy metal contaminated groundwater. J. Environ. Manag.
484 doi:10.1016/j.jenvman.2011.06.009
485 Hedin, R.S., G.R. Watzlaf, and R.W. Nairn. 1994. Passive Treatment of Acid-Mine
486 Drainage with Limestone. J. Environ. Qual. 23, 1338-1345.
487 Hedin, R.S., 2008. Iron Removal by a Passive System Treating Alkaline Coal Mine
488 Drainage. Mine Water Environ. 27, 200-209.
489 Jage, C.R., C.E. Zipper, and R. Noble. 2001. Factors affecting alkalinity generation by
490 successive alkalinity-producing systems: Regression analysis. J. Environ. Qual.
491 30, 1015-1022.
492 Johnson, D.B., Hallberg, K.B., 2005. Acid mine drainage remediation options: a review.
493 Sci. Total Environ. 338 (1-2), 3-14.
494 Johnson, D.B., Hallberg, K.B., 2003. The microbiology of acidic mine waters. Res.
495 Microbiol. 154 (7), 466-473.
496 Kalin, M., 2004. Passive mine water treatment: the correct approach? Ecol. Eng. 22,
497 299-304.
498 Kirby, C.S., Cravotta, C.A., 2005a. Net alkalinity and net acidity 1: Theoretical
499 considerations. Appl. Geochem. 20 (10), 1920-40.

500 Kirby, C.S., Cravotta, C.A., 2005b. Net alkalinity and net acidity 2: Practical
501 considerations. Appl. Geochem. 20 (10), 1941-1964.
502 Kirby, C.S., Thomas, H.M., Southam, G., Donald, R., 1999. Relative contributions of
503 abiotic and biological factors in Fe(II) oxidation in mine drainage. Appl.
504 Geochem. 14 (4), 511-530.
505 Kruse, N.A.S., Gozzard, E., Jarvis, A.P., 2009. Determination of Hydraulic Residence
506 Times in Several UK Mine Water Treatment Systems and their Relationship to
507 Iron Removal. Mine Water Environ. 28, 115-123.
508 Long, Z., Huang, Y., Cai, Z., Cong, W., Ouyang, F., 2003. Biooxidation of ferrous iron
509 by immobilized Acidithiobacilus ferrooxidans in poly (vinyl alcohol) cryogel
510 carriers. Biotechnol. Lett. 25, 245-249.
511 López Fernández, A., López Montenegro, G., Romero Sousa, J., 2003. Tratamiento de
512 aguas de Minería en el río Odiel, Medio Ambiente.
513 Mayes, W.M., Batty, L.C., Younger, P.L., Jarvis, A.P., Koiv, M., Vohla, C., et al. 2009.
514 Wetland treatment at extremes of pH: A review. Sci. Total. Environ. 407 (13),
515 3944-3957.
516 Nyquist, J., Greger, M., 2009. A field study of constructed wetlands for preventing and
517 treating acid mine drainage. Ecol. Eng. 35, 630-642.
518 Olías, M., Cánovas, C.R., Nieto, J.M., Sarmiento, A.M., 2006. Evaluation of the
519 dissolved contaminant load transported by the Tinto and Odiel rivers (South
520 West Spain). Appl. Geochem. 21, 1733-1749.
521 Parkhurst, D.L., Appelo, C.A.J., 1999. User's Guide to PHREEQC (Version 2) A
522 Computer Program for Speciation, Batch-Reaction, One-Dimensional Transport,
523 and Inverse Geochemical Calculations, USGS Water-Resources Investigations,
524 Denver, Colorado.

525 Pinedo Vara, I., 1963. Piritas de Huelva. Su Historia, Minería y Aprovechamiento, In:
526 Summa, Madrid.
527 PIRAMID-Consortium., 2003. Engineering guidelines for the passive remediation of
528 acidic and/or metalliferous mine drainage and similar wastewaters. European
529 Commission 5th Framework RTD Project no. EVK1-CT-1999-000021 "Passive
530 in-situ remediation of acidic mine / industrial drainage" (PIRAMID). University
531 of Newcastle Upon Tyne, Newcastle Upon Tyne UK.
532 Rodier, J., Broutin, J.P., Chambon, P., Champsaur, H., Rodi, L., 1996. L'analyse de
533 l'eau, Dunod, Paris.
534 Rötting, T.S., Ayora, C., Carrera, J., 2005. Passive treatment of Acid Mine Drainage
535 with high metal concentrations: Results from experimental treatment tanks in the
536 Iberian Pyrite Belt (SW Spain). Proceedings of the 9th International Mine Water
537 Association Congress, Oviedo, Spain. p. 641-647.
538 Rötting, T.S., Thomas, R.C., Ayora, C., Carrera, J., 2008a. Passive Treatment of Acid
539 Mine Drainage with High Metal Concentration Using Dispersed Alkaline
540 Substrate. J. Environ. Qual. 37, 1741-1751.
541 Rötting, T.S., Caraballo, M.A., Serrano, J.A., Ayora, C., Carrera, J., 2008b. Field
542 application ofcalcite Dispersed Alkaline Substrate (calcite-DAS) for passive
543 treatment of acid mine drainage with high Al and metal concentrations. Appl.
544 Geochem. 23 (6), 1660-1674.
545 Rötting, T.S., Ayora, C., Carrera, J., 2008c. Improved passive treatment of high Zn and
546 Mn concentrations using Caustic Magnesia (MgO): Particle size effects.
547 Environ. Sci. Technol. 24 (42), 9370–9377.

548 Sáinz, A., Grande, J.A., de la Torre, M.L., Sánchez-Rodas D., 2002. Characterisation of
549 sequential leachate discharges of mining waste rock dumps in the Tinto and
550 Odiel rivers. J. Environ. Manag. 64, 345-353.
551 Sapsford, D.J., Watson, I., A process-orientated design and performance assessment
552 methodology for passive mine water treatment systems. Ecol. Eng. (2011), doi:
553 10.1016/j.ecoleng.2010.12.010
554 Sarmiento, A.M., Nieto, J.M., Olías, M., Cánovas, C.R., 2009. Hydrochemical
555 characteristics and seasonal influence on the pollution by acid mine drainage In
556 the Odiel river Basin (SW Spain). Appl. Geochem. 24, 697-714.
557 Singer, P.C., and Stumm, W., 1970. Acidic Mine Drainage . The Rate-Determining
558 Step. Science 167, 1121-1123.
559 Tyler, G., Carrasco, R., Nieto, J.M., Pérez, R., Ruiz, M.J., Sarmiento, A.M. 2004.
560 Optimization of major and trace element determination in acid mine drainage
561 samples by ultrasonic nebulizer-ICP-OES (USN-ICP-OES). In: Pittcon
562 conference, Chicago, USA.
563 Whitehead, P.G., Hall, G., Neal, C., Prior, H., 2005. Chemical behavior of the Wheal
564 Jane bioremediation system. Sci. Total Environ. 338 (1-2), 41-51.
565 Younger, P.L., Banwart, S.A., Hedin, R.S., 2002. Mine Water - Hydrology, Pollution,
566 Remediation. Kluwer Academic Publishers, Dordrecht.
567 Younger, P.L., 2000. The Adoption and Adaptation of Passive Treatment Technologies
568 for Mine Waters in The United Kingdom. Mine Water Environ. 19 (2), 84-97.
569 Ziemkiewicz, P.F., Skousen, J.G., Simmons, J., 2003. Long-term Performance of
570 Passive Acid Mine Drainage Treatment Systems. Mine Water Environ. 22 (3),
571 118-129.

572
573

FIGURE CAPTIONS

Figure 1. General (A) and detailed (B) field site location and schematic view of the DAS passive treatment system (C).

Figure 2. Example of typical Fe-stromatolites forming cascades and pools (A). Detail of the Fe-stromatolites developed close to the mine shaft of Monte Romero (B) and general view of the NFOL pretreatment (C).

Figure 3. Time evolution of Fe speciation in both shaft and lagoon.

Figure 4. Fe, Al, pH and alkalinity (mg/L as $CaCO_3$ equivalents) distribution along the main representative points of the treatment (May 2008). T*n*-in: tank *n* inflow, T*n*-out: tank *n* outflow, D*n*-out: decantation pond *n* outflow.

Figure 5. Fe, Al, Zn, Cu, As and Pb metal removal reported by Rötting et al. (2008b) (A), Caraballo et al. (2009a) (B) and this study (C). Numbers in percentage correspond to the removal for each metal and section. Section 1: NFOL pretreatment, Section 2: first limestone-DAS tank and two decantation ponds; and Section 3: second limestone-DAS tank. The data are presented in three bars for each metal. Within the bars the removal percentage for each section related to the metal content at the mine shaft is indicated. The sum of these percentages indicates the total removal achieved for each metal and experiment.

TABLES

Table 1. AMD mean elements concentration, pH, Eh and SI values, at representative points of the treatment. SI calculated using PHREEQC and Wateq4F database. Only typical mineral phases in AMD environments are shown.

Table 2. Chemical composition (mg/g) of the solid samples from the NFOL and both limestone-DAS tank depth profiles.

Table 3. Design parameters and Fe removal rates reported for different passive treatment systems and water compositions.

Figure 1

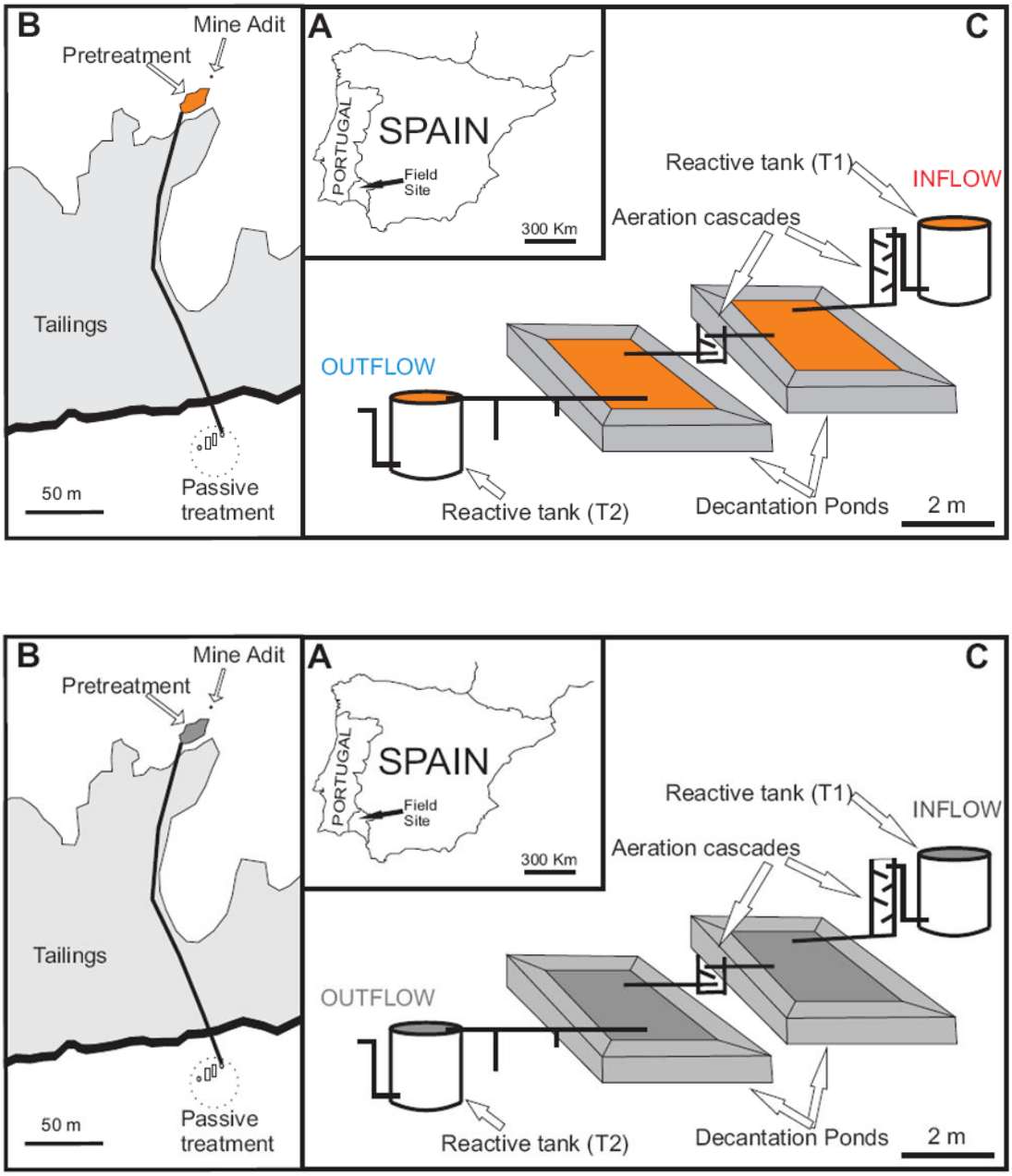
B
Mine Adit
Pretreatment
Tailings
50 m
Passive
treatment
A
PORTUGAL
SPAIN
Field
Site
300 Km
C
Reactive tank (T1)
INFLOW
Aeration cascades
OUTFLOW
Reactive tank (T2)
Decantation Ponds
2 m
B
Mine Adit
Pretreatment
Tailings
50 m
Passive
treatment
A
PORTUGAL
SPAIN
Field
Site
300 Km
C
Reactive tank (T1)
INFLOW
Aeration cascades
OUTFLOW
Reactive tank (T2)
Decantation Ponds
2 m

Figure 2

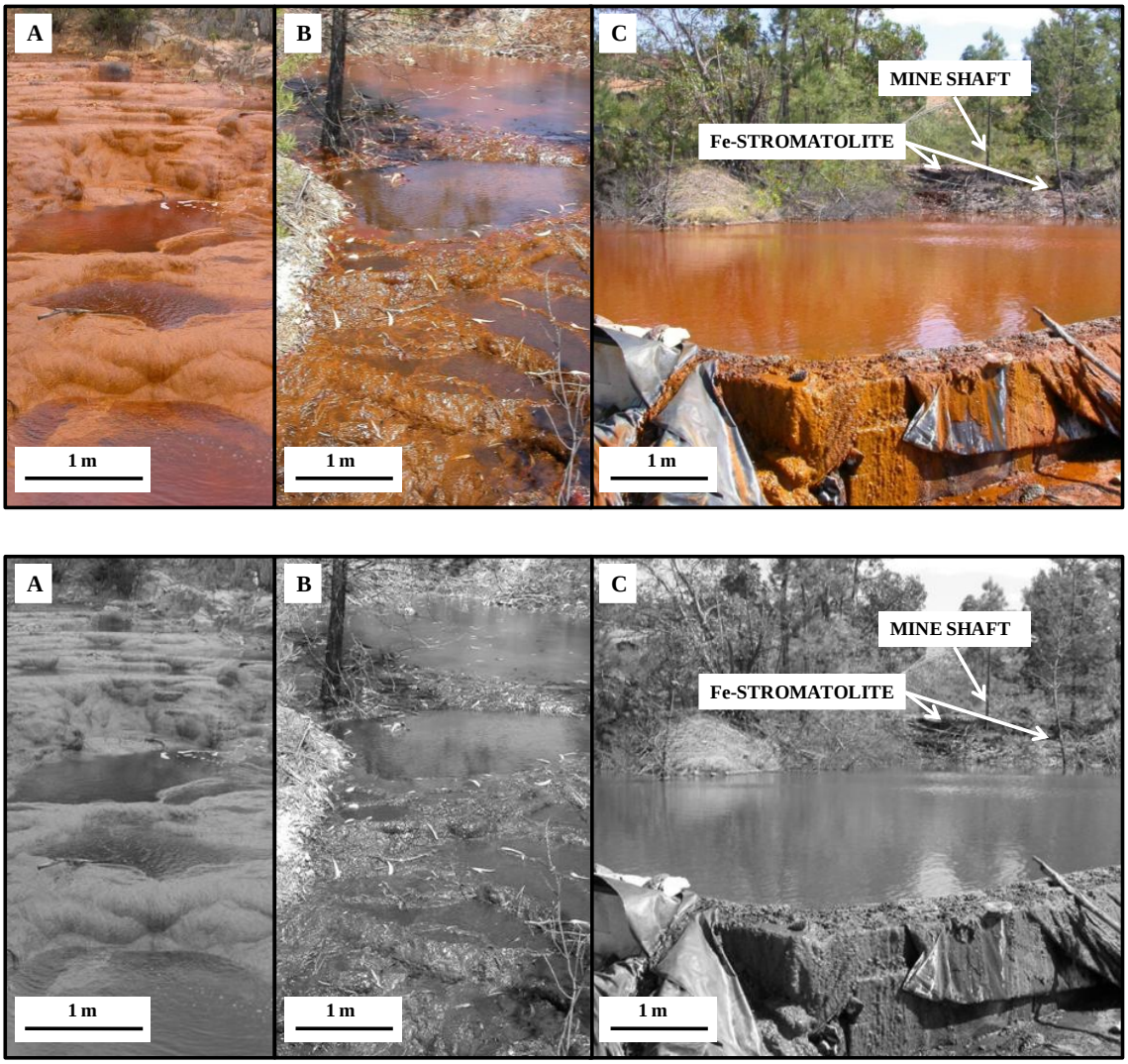
A
B
C
MINE SHAFT
Fe-STROMATOLITE
1 m
1 m
1 m
A
B
C
MINE SHAFT
Fe-STROMATOLITE
1 m
1 m
1 m

Figure 3

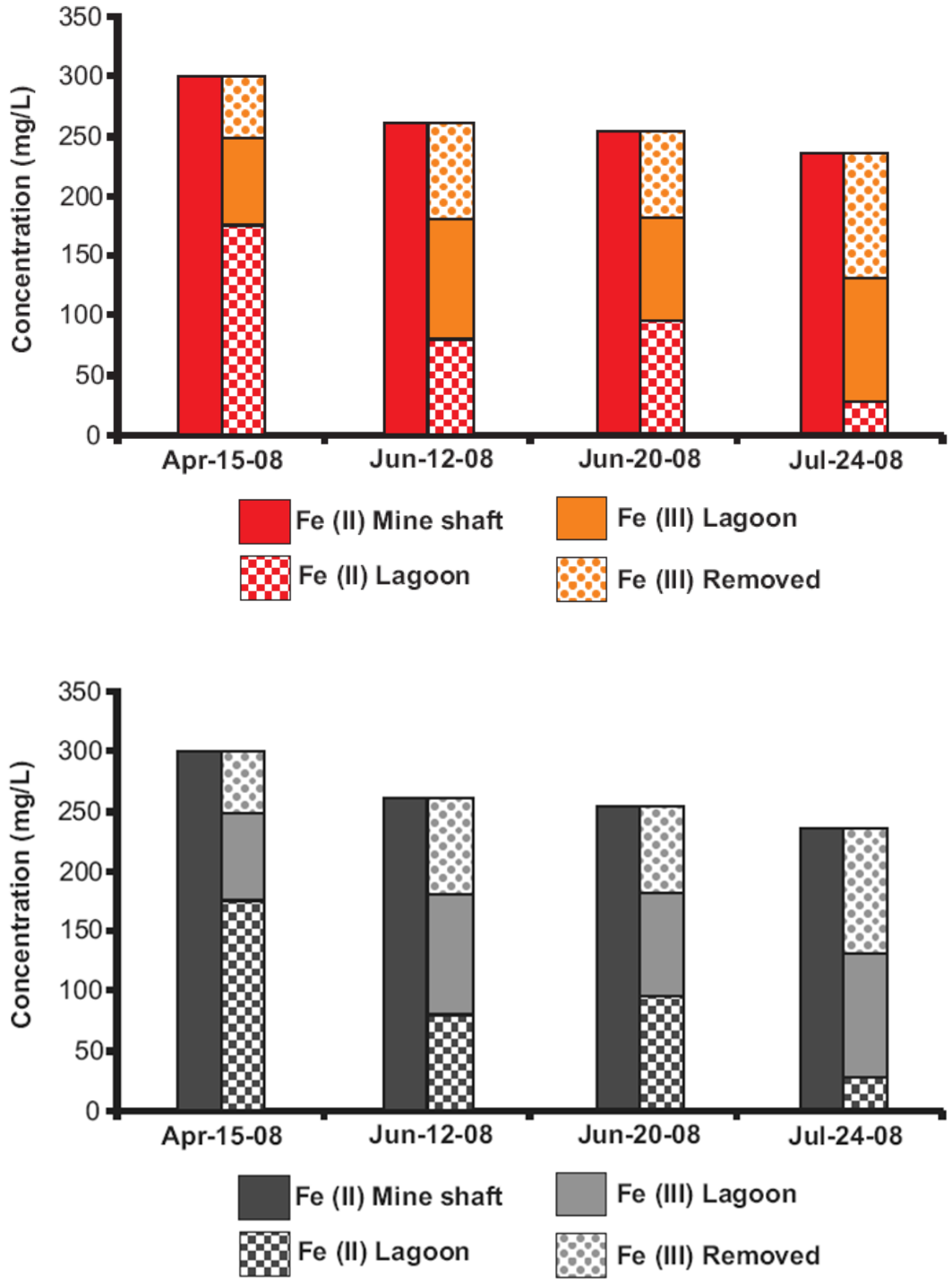
Concentration (mg/L)
350
300
250
200
150
100
50
0
Apr-15-08
Jun-12-08
Jun-20-08
Jul-24-08
Fe (II) Mine shaft
Fe (II) Lagoon
Fe (III) Lagoon
Fe (III) Removed
Concentration (mg/L)
350
300
250
200
150
100
50
0
Apr-15-08
Jun-12-08
Jun-20-08
Jul-24-08
Fe (II) Mine shaft
Fe (II) Lagoon
Fe (III) Lagoon
Fe (III) Removed

Figure 4

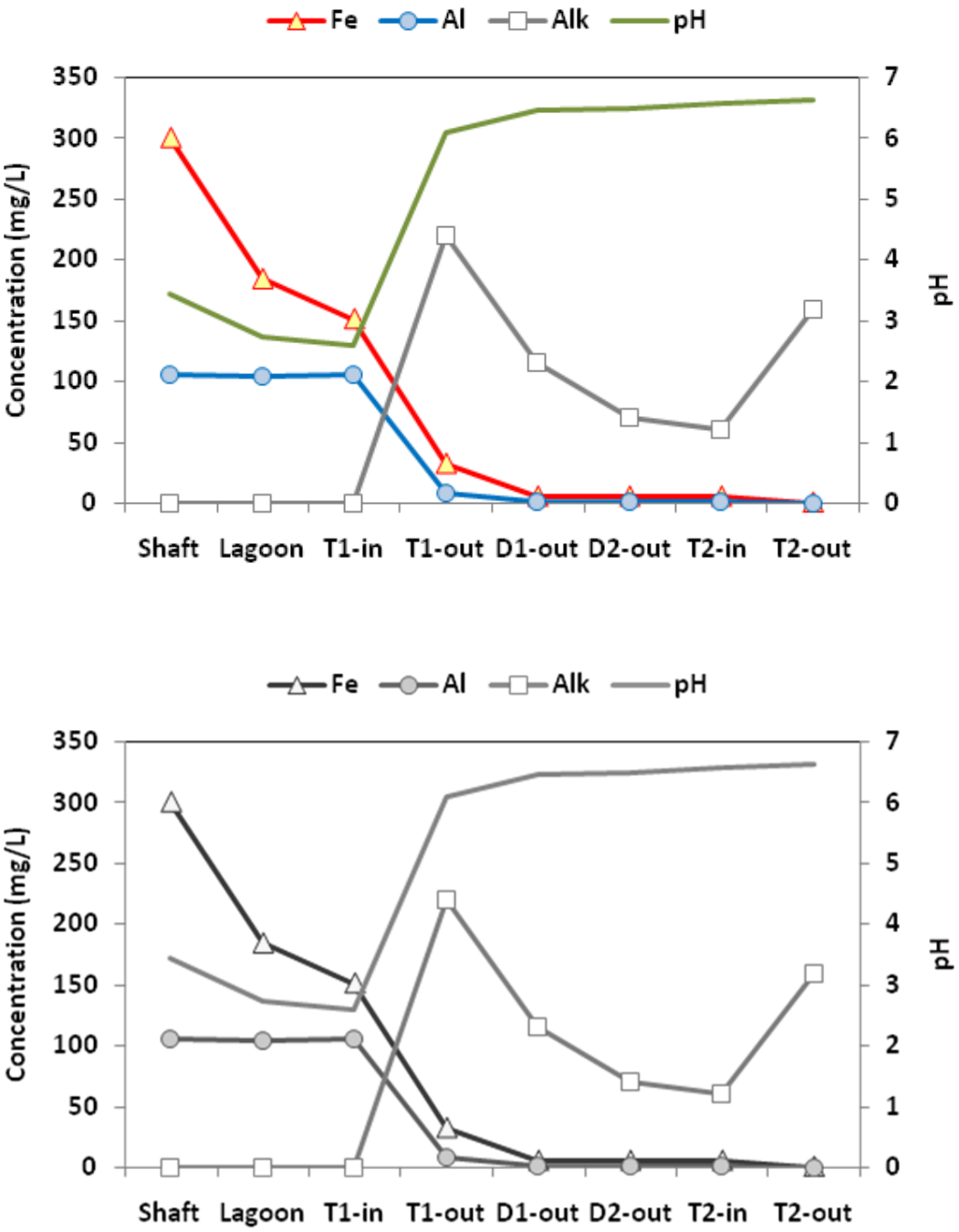
Fe
Al
Alk
pH
Concentration (mg/L)
pH
350
300
250
200
150
100
50
0
7
6
5
4
3
2
1
0
Shaft
Lagoon
T1-in
T1-out
D1-out
D2-out
T2-in
T2-out

Figure 5

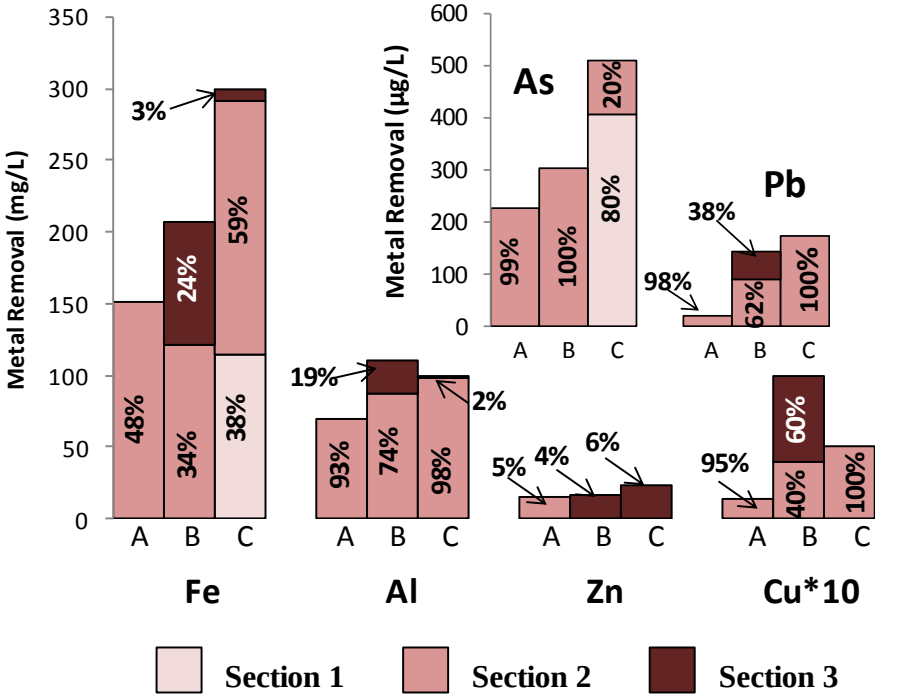
Metal Removal (mg/L)
Metal Removal (µg/L)
Fe
Al
Zn
Cu*10
As
Pb
Section 1
Section 2
Section 3

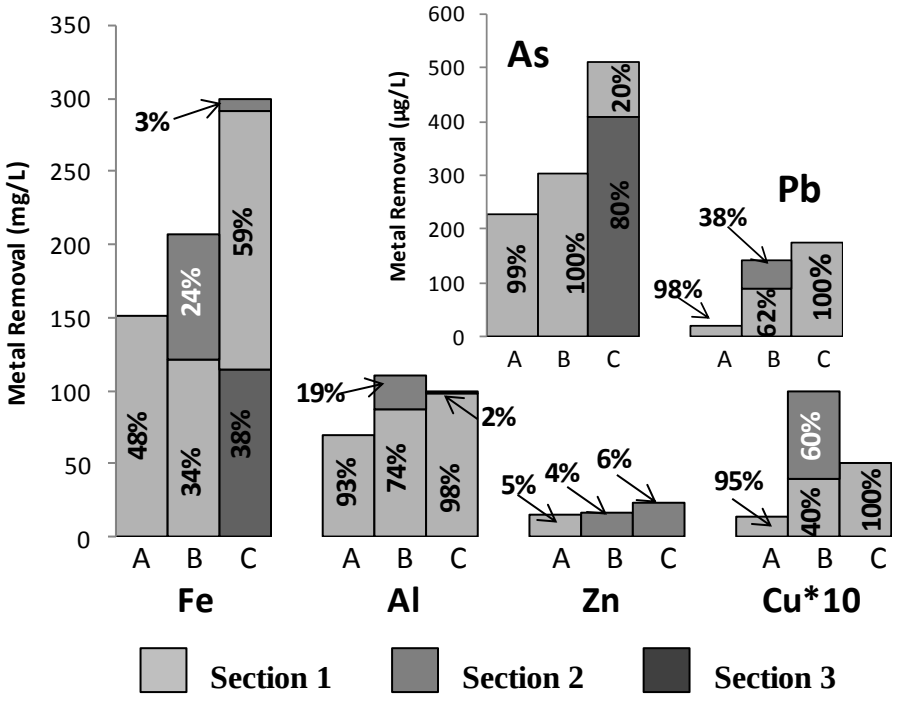
Metal Removal (mg/L)
Metal Removal (µg/L)
Fe
Al
Zn
Cu*10
As
Pb
Section 1
Section 2
Section 3

Table 1

Table 1.
AMD mean elements concentration, pH, Eh and SI values, at representative points of the treatment. SI calculated using PHREEQC and Wateq4F database. Only typical mineral phases in AMD environments are shown.

	pH	Eh	mg/L										µg/L		SI						
			Fe	Al	SO_4	Ca	Zn	Cu	K	Mg	Mn	Si	As	Pb	Al $(OH)_3$	Basal	Gib	Fe $(OH)_3$	Schw	Gth	Gyp
Shaft	3	508	275	100	3430	250	440	5	5	255	18	37	507	174	-5.0	-8.2	-2.3	-2.2	-5.0	3.6	-0.3
NFOL	2.7	653	171	100	3440	252	443	5	3	263	18	38	97	182	-6.4	-13.1	-3.7	-1.3	3.9	4.5	-0.3
T1 out	6.1	299	15	10	3590	810	436	n.d.	4	279	19	19	n.d.	n.d.	1.1	10.8	3.8	1.9	18.4	7.8	0.2
D2 out	6	356	5	10	3870	790	430	n.d.	7	316	18	18	n.d.	n.d.	0.7	9.7	3.4	0.2	5.9	6.1	0.1
T2 out	6.6	341	n.d.	n.d.	3770	850	414	n.d.	7	386	19	11	n.d.	n.d.	n.c	n.c	n.c	n.c	n.c	n.c	0.2

The major elements concentration (mg/L) corresponds to a 99% of the total element concentration in the samples. $Al(OH)_3$: $Al(OH)_3$ amorphous, Basal: Basaluminite, Gib: Gibbsite, $Fe(OH)_3$: $Fe(OH)_3$ amorphous, Schw: Schwertmannite, Gth: Goethite, Gyp: Gypsum. n.c (not calculated). n.d. (not detected). AMD: acid mine drainage, SI: saturation index.

Table 2

Table 2.
Chemical composition (mg/g) of the solid samples from the NFOL and both limestone-DAS tank depth profiles

	Fe	S	Al	Ca	Zn	Cu	As	Pb
NFOL	360.07	44.03	0.45	0.10	0.24	-	0.84	-
Depth T1 (cm)								
0-1	339.72	42.79	0.97	51.44	1.24	0.31	0.40	-
1-6	67.56	22.17	25.33	118.14	3.06	0.32	0.02	0.04
6-11	2.15	10.68	24.82	224.41	5.8	0.82	-	-
11-16	-	7.82	18.77	245.07	2.6	0.86	-	-
16-21	-	0.59	4.25	304.92	1.01	0.41	-	-
21-26	-	0.37	1.32	323.61	0.86	0.44	-	-
26-31	-	-	1.32	271.53	1.32	0.53	-	-
31-36	-	-	0.68	294.45	0.91	0.19	-	-
36-45	-	-	0.47	262.28	1.08	0.13	-	-
Depth T2 (cm)								
0-2	28.53	147.78	8.45	198.34	18.32	-	-	-
2-10	12.95	6.42	3.69	285.05	33.71	-	-	-
10-20	2.36	1.87	0.41	338.13	7.38	-	-	-
20-30	0.91	0.83	0.30	331.22	3.85	-	-	-
30-40	0.45	0.38	-	341.63	1.55	-	-	-

NFOL: natural Fe-oxidizing lagoon

Table 3

Table 3.
Design parameters and Fe removal rates reported for different passive treatment systems and water compositions

	Inflow rate (L/s)	Area (m^2)	Influent (mg/L)	Removal ($g/m^2/day$)	References
Settlement Lagoons (recommendations)	100 m^2 of lagoon area per 1L/s flow		< 50	10	PIRAMID-consortium (2003)
Aerobic Wetland (recommendations)	Area depends on flow-rate and influent/ effluent Fe		5-50	10-20	PIRAMID-consortium (2003)
Lagoons/ponds (alkaline waters)	5-6000	375-21000	28-74	16-26	Kruse et al. (2009) Hedin (2008)
Aerobic wetlands (acid waters)	0.3	8175	143	6	Whitehead et al. (2005)
NFOL	1.5	100	265	100	This study

NFOL: natural Fe-oxidizing lagoon